

## Comparison of LCModel and SAGE in Analysis of Brain Metabolite Concentrations-A study of Patients with Mild Cognitive Impairment

Chiu-Ming Shih<sup>1</sup>, Jui-Jen Lai<sup>1</sup>, Chin-Ching Chang<sup>1</sup>, Cheng-Sheng Chen<sup>3</sup>, Yi-Chun Yeh<sup>3</sup>,  
Twei-Shiun Jaw<sup>1</sup>, Jui-Sheng Hsu<sup>1</sup>, Chun-Wei Li<sup>2\*</sup>

### Abstract-

**Purpose:** The purpose of this study was to compare brain metabolite concentration ratios determined by LCModel and Spectroscopy Analysis by General Electric (SAGE) quantitative methods to elucidate the advantages and disadvantages of each method.

**Materials and Methods:** A total of 10 healthy volunteers and 10 patients with mild cognitive impairment (MCI) were recruited in this study. A point-resolved spectroscopy (PRESS) sequence was used to obtain the brain magnetic resonance spectroscopy (MRS) spectra of the volunteers and patients, as well as the General Electric (GE) MRS-HD-sphere phantom. The brain metabolite concentration ratios were estimated based on the peak area obtained from both LCModel and SAGE software. Three brain regions were sampled for each volunteer or patient, and 20 replicates were acquired at different times for the phantom analysis.

**Results:** The metabolite ratios of the GE phantom were estimated to be myo-inositol (mI)/creatine (Cr):  $0.70 \pm 0.01$ , choline (Cho)/Cr:  $0.37 \pm 0.00$ , N-acetylaspartate (NAA)/Cr:  $1.26 \pm 0.02$ , and NAA/mI:  $1.81 \pm 0.04$  by LCModel, and mI/Cr:  $0.88 \pm 0.15$ , Cho/Cr:  $0.35 \pm 0.01$ , NAA/Cr:  $1.33 \pm 0.03$ , and NAA/mI:  $1.55 \pm 0.26$  by SAGE. In the healthy volunteers and MCI patients, the ratios of mI/Cr and Cho/Cr estimated by LCModel were higher than those estimated by SAGE. In contrast, the ratio of NAA/Cr estimated by LCModel was lower than that estimated by SAGE.

**Conclusion:** Both methods were acceptable in estimating brain metabolite concentration ratios. However, LCModel was marginally more accurate than SAGE because of its full automation, basis set, and user independency.

**Abbreviations:** NAA, N-acetylaspartate; Cr, creatine; Cho, choline; mI, myo-inositol; MCI, mild cognitive impairment; SAGE, Spectroscopy Analysis by General Electric; PRESS, point-resolved spectroscopy; MRS, magnetic resonance spectroscopy; Alzheimer's disease (AD); DLPL, dorsolateral prefrontal lobe

*Acta Neurol Taiwan 2017;26:20-28*

From the <sup>1</sup>Department of Medical Imaging Kaohsiung Medical University Hospital, Kaohsiung, Taiwan; <sup>2</sup>Department of Medical Imaging and Radiological Sciences, Kaohsiung Medical University; Department of <sup>3</sup>Psychiatry, Chung-Ho Memorial Hospital, Kaohsiung Medical University.  
Received December 23, 2015.  
Revised & Accepted February 22, 2017.

Correspondence to: Chun-Wei Li, PhD. Department of Medical Imaging and Radiological Sciences Kaohsiung Medical University, 100, Shih-Chuan 1st Road, Kaohsiung, 80708, Taiwan.  
E-mail: cw10331@gmail.com

## INTRODUCTION

Magnetic resonance spectroscopy (MRS) is a non-invasive technique that has been used to estimate changes in the metabolite:creatine-phosphocreatine (Cr) concentration ratios. This can be used to study numerous diseases, such as brain tumors, strokes, seizure, Alzheimer's disease (AD), and other diseases affecting the brain<sup>(1)</sup>. MRS can be used to determine the amount of cerebral metabolites, including N-acetylaspartate (NAA), choline-containing compounds (Cho), creatine-phosphocreatine (Cr), and myo-inositol (mI) in the brain. NAA, which is synthesized from amino acids, is contained in the mitochondria of nerve cells. Its concentration is positively correlated to that of oxygen consumed by the brain cells and negatively correlated to the extent of neuronal injury or loss, serving as an indicator of neuronal density<sup>(2-7)</sup>. Cr is a relatively stable metabolite in the brain and is commonly used as the internal standard to normalize the concentration of other metabolites measured by MRS<sup>(2,3,4,8)</sup>. Cho is one of the main components of brain cell membranes, wherein mI, a sugar-alcohol, is also contained. Thus, the intensity of the Cho peak can be used as an indicator of cellular density and membrane turnover<sup>(2,4,7,8)</sup>. The peak intensity of mI can be used to indicate glial cell number because of its high concentration in glial cells. Variations in mI levels have been reported in patients with mild cognitive impairment (MCI), AD, or dementia disease<sup>(9-12)</sup>. So, far, there are no effective ways to cure such diseases. Thus, early diagnosis of dementia syndromes before onset is critical.

MCI patients with memory loss but normal cognitive function have a much higher risk of developing diseases causing dementia compared to normal individuals of the same age. The risk of developing AD is also high in MCI patients<sup>(13,14)</sup>. MRS is capable of detecting changes in the brain concentration of NAA, Cho, Cr, and mI, and these changes can be used to predict whether MCI disease will progress to AD or other diseases causing dementia<sup>(15,16)</sup>. However, the MRS quantification method has two major drawbacks: highly complicated spectra that are hard to resolve and unpredictable peak profiles and baselines. The inhomogeneity of the magnetic field caused by incomplete shimming increases the peak width, resulting in severe peak overlap that affects the precision and accuracy of the

calculation for metabolite concentrations.

The LCModel method is used to calculate metabolite concentrations in vivo based on model spectra derived from individual metabolites in vitro. Using the whole standard spectra rather than the individual peaks, two overlapping spectra belonging to different metabolites in the same frequency region can be resolved. Furthermore, unpredictable variations in the peak profile caused by eddy currents, inhomogeneous magnetic fields, short echo times, and fat or macromolecular resonances, which are hard to control in vivo, can easily be differentiated by comparing the patterns of the whole spectra.

SAGE 7.6 (Spectroscopy Analysis by General Electric) is a spectroscopic processing and display software tool made by GE<sup>(17)</sup>. It provides a powerful toolkit to handle a wide variety of tasks associated with spectroscopy data management and quantitation. It processes the MRS data in fully artificial steps that include apodization, zero filling, Fourier Transform, phase adjusting, baseline correction, and Fitting.

The purpose of this study was to compare the advantages and disadvantages of LCModel and SAGE based on the evaluated brain metabolite concentration ratios determined by each method.

## MATERIALS AND METHODS

Under the approval of the local Ethics Committee, 10 healthy volunteers (females, 5; males, 5; age range, 65–82 years; median age, 67 years) and 10 MCI patients (female, 1; male 9; age range, 54–74 years; median age, 65 years) were recruited for this study. The assessment of MCI patients included memory, executive function (Trail Making Test), attention (digit span forward), language (Naming Test, letter and category fluency) and visuospatial (figure copying). After three-plane scout views, T2 FIAIR images in the axial plane and T1-weighted images in the coronal plane were obtained for localizing the proton-MRS (1H MRS) voxel. Single-voxel point-resolved spectroscopy (PRESS) pulse sequence (TR/TE 1500/30 ms, BW 1000 Hz, 1024 points, 128 excitations) was used to obtain the spectra of the GE MRS-HD-sphere phantom, healthy volunteers, and MCI patients. In the phantom test, the experiment was repeated 20 times in different periods of time using a 3T GE Signa VH/i MR system.

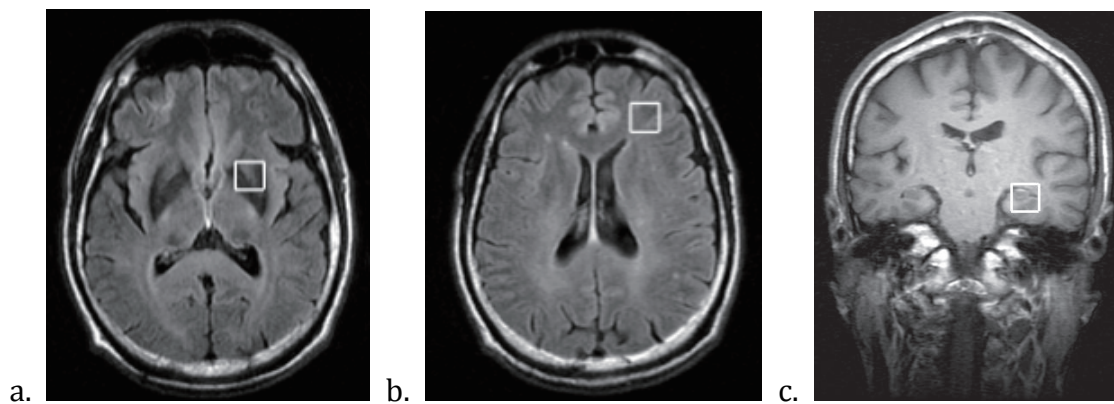
The prescan algorithm of PROBE automatically adjusts the transmitter and receiver gains and center frequency. The local magnetic field homogeneity was optimized by auto-shim procedure, and chemical-shift-water suppression (CHESS) sequence was executed prior to PRESS acquisition to suppress the water signal. The voxel size was  $15 \times 15 \times 15 \text{ mm}^3$ . Spectra were taken from the spatial region of the basal ganglia, dorsolateral prefrontal lobe (DLPL), and hippocampus, as shown in Figure 1. LCModel and SAGE softwares were used to estimate the metabolite concentrations. There are no corrections for relaxation in both software analyses; because of the relaxation effects partially cancel in concentration ratios. In the SAGE analysis, the raw data were zero-filled once, apodized with a 3-Hz Gaussian filter, Fourier transformed, and phase and baseline corrected. Marquardt curve fitting was performed based on a Gaussian shape to calculate

the peak area. The metabolite concentration ratios were calculated using the concentration of Cr, which is a physiologically stable metabolite, as the reference. Paired t-test was used to compare the ratios calculated by the two methods using SPSS 21 package, and  $p < 0.05$  was used to indicate statistically significant differences.

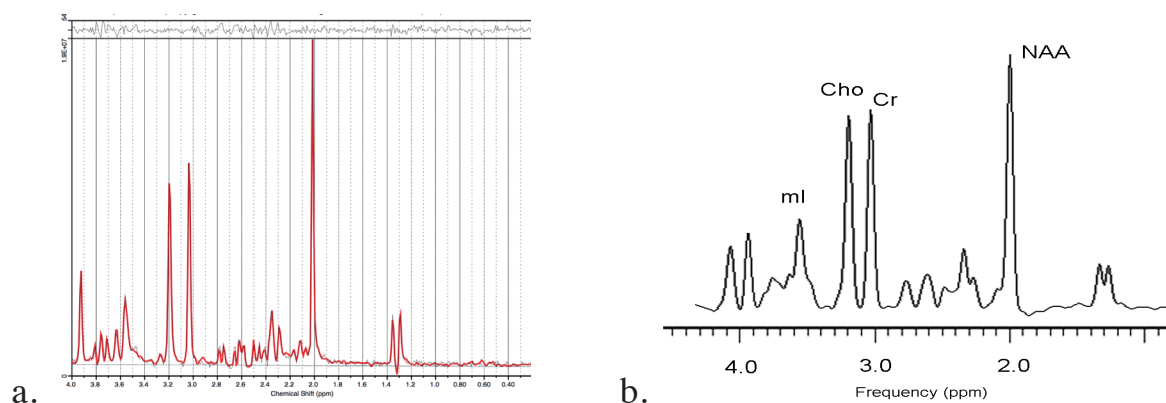
## RESULTS

Figure 1 illustrates the location of the voxel of interest (VOI) in the basal ganglia, DLPL, and hippocampus. Figures 2–5 show the data calculated from the spectra acquired from the phantom, basal ganglia, DLPL, and hippocampus by LCModel and SAGE. Figure 6 shows the scatter plot of the four metabolites ratios calculated by LCModel and SAGE from the phantom.

The metabolite ratios (Mean  $\pm$  SD) and statistical



**Figure 1.** The location of the voxel of interest (VOI) in the basal ganglia and the dorsolateral prefrontal lobe on axial T2-weighted imaging (a), (b), and the location of the VOI in the hippocampus on coronal T1-weighted imaging (c).



**Figure 2.** Spectrum of the phantom analysis from (a) LCModel and (b) SAGE with line broadening equal to 3 Hz

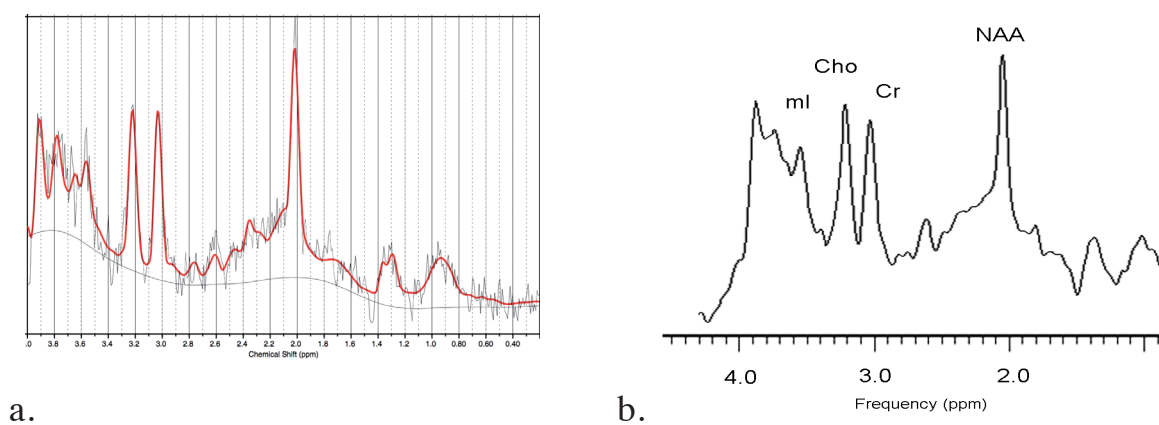


**Figure 3.** Spectrum of the basal ganglia analysis from (a) LCMoDel and (b) SAGE with line broadening equal to 3 Hz

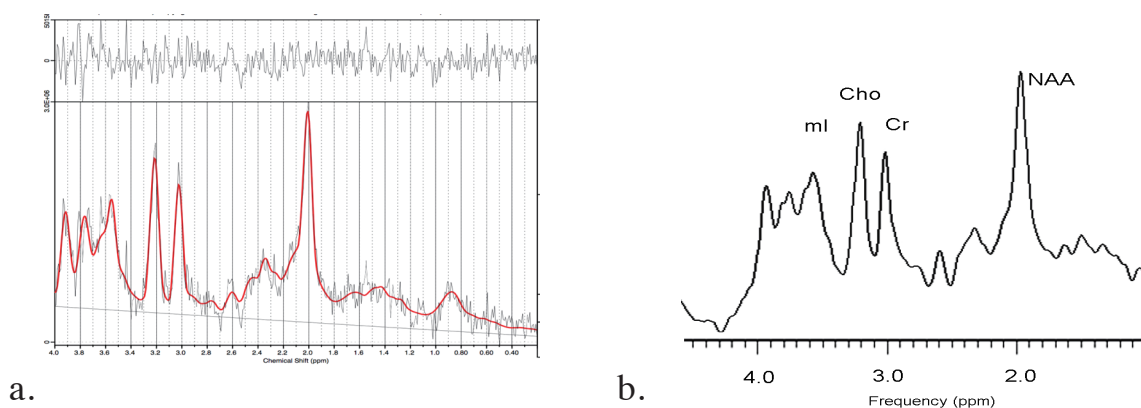


**Figure 4.** Spectrum of the dorsolateral prefrontal lobe analysis from (a) LCMoDel and (b) SAGE with line broadening equal to 3 Hz

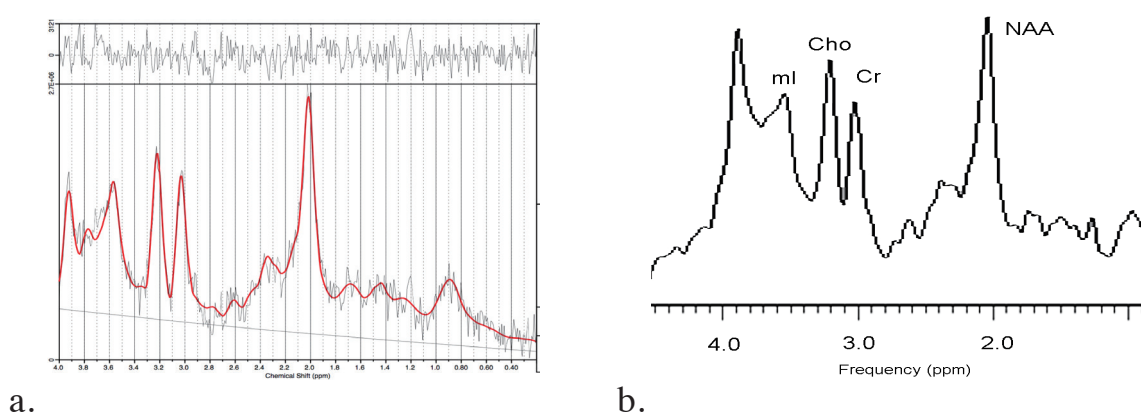


**Figure 5.** Spectrum of the hippocampus from (a) LCMoDel and (b) SAGE with line broadening equal to 3 Hz

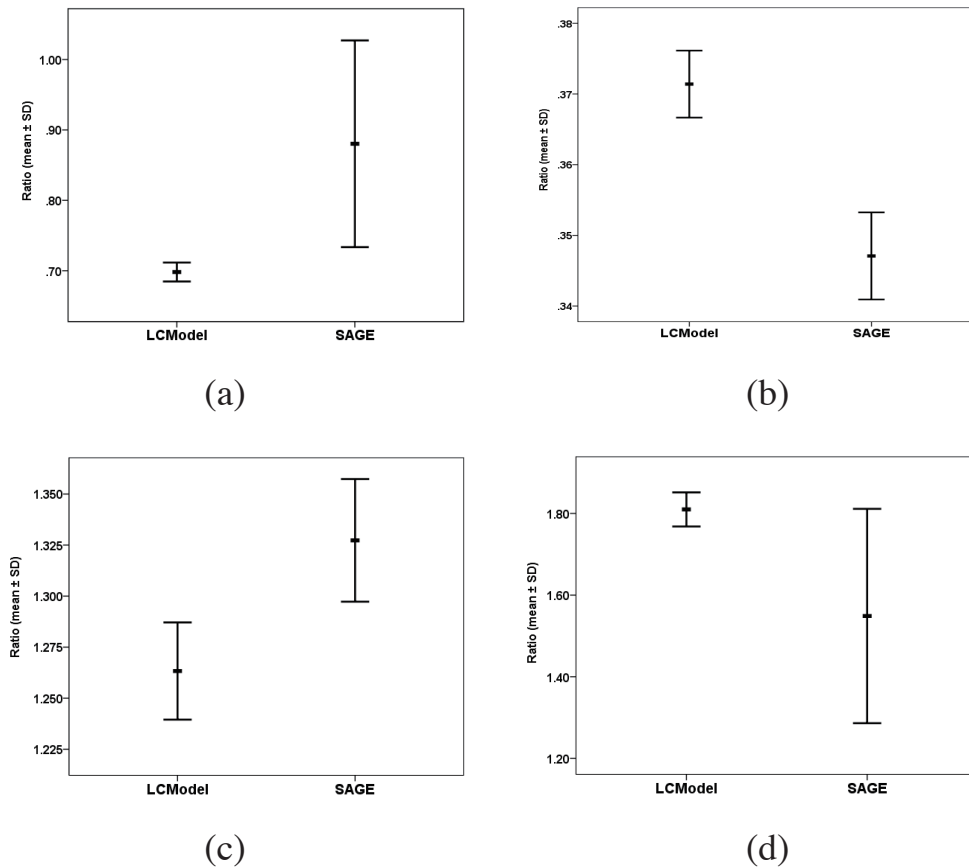


**Figure 6.** Error bar charts of the metabolite ratios by LCMoel and SAGE in the phantom analysis (a) mI/Cr, (b) Cho/Cr, (c) NAA/Cr, (d) NAA/mI

significance of the concentration ratios calculated from the phantom and the basal ganglia, DLPL, and hippocampus of the healthy volunteers and MCI patients are shown in Tables 1, 3, and 4. The difference of metabolite ratio of the true concentration and obtained by the two software analyzes and their statistical significance are show in Table 2.

In the phantom experiment, the mI/Cr and NAA/Cr ratios obtained by LCMoel were lower than those obtained by SAGE, and the Cho/Cr and NAA/mI ratios obtained by LCMoel were higher than those obtained by

SAGE (Table 1). In the three regions of the brain in the healthy volunteers and the MCI patients, the mI/Cr and Cho/Cr values estimated by LCMoel were higher than those estimated by SAGE. In contrast, the NAA/Cr ratios estimated by LCMoel were lower than those estimated by SAGE (Table 3 and 4).

In the phantom, significant differences ( $p < 0.05$ ) between ratios determined by the two methods were found for all metabolite ratios. In healthy volunteers, except for mI/Cr and Cho/Cr in the basal ganglia and Cho/Cr in the DLPL, significant differences ( $p < 0.05$ ) were found

**Table 1.** Metabolite ratios (Mean  $\pm$  SD) and their statistical significance in the phantom analysis

Phantom	LCMoel	SAGE	P value
mI/Cr	$0.7 \pm 0.01$	$0.88 \pm 0.15$	$< 0.001$
Cho/Cr	$0.37 \pm 0.00$	$0.35 \pm 0.01$	$< 0.001$
NAA/Cr	$1.26 \pm 0.02$	$1.33 \pm 0.03$	$< 0.001$
NAA/mI	$1.81 \pm 0.04$	$1.55 \pm 0.26$	$< 0.001$

**Table 2.** The difference of metabolite ratio of the real concentration and obtained by the two software analyzes and their statistical significance

Metabolites	Phantom	LCModel	SAGE	P value
mI/Cr	0.75	0.06 ± 0.03	0.15 ± 0.12	< 0.057
Cho/Cr	0.3	0.03 ± 0.01	0.05 ± 0.01	< 0.000
NAA/Cr	1.25	0.02 ± 0.01	0.08 ± 0.03	0.001
NAA/ml	1.67	0.1 ± 0.04	0.23 ± 0.17	0.01

**Table 3.** Metabolite ratios (Mean ± SD) and their statistical significance in the basal ganglia, the dorsolateral prefrontal lobe, and the hippocampus of healthy volunteers

Basal ganglia		LCModel	SAGE	P value
	mI/Cr	0.66 ± 0.37	0.42 ± 0.26	0.11
	Cho/Cr	0.30 ± 0.08	0.24 ± 0.18	0.07
	NAA/Cr	0.97 ± 0.27	2.52 ± 0.87	< 0.001
	NAA/ml	1.77 ± 0.9	8.45 ± 6.08	< 0.001
Dorsolateral prefrontal lobe	mI/Cr	1.06 ± 0.32	0.35 ± 0.28	< 0.001
	Cho/Cr	0.32 ± 0.03	0.30 ± 0.11	0.62
	NAA/C	1.29 ± 0.26	2.14 ± 0.62	< 0.001
	NAA/ml	1.27 ± 0.25	11.24 ± 12.45	< 0.001
Hippocampus	mI/Cr	1.13 ± 0.22	0.77 ± 0.40	0.02
	Cho/Cr	0.36 ± 0.05	0.29 ± 0.07	< 0.001
	NAA/Cr	1.03 ± 0.28	2.78 ± 0.67	< 0.001
	NAA/ml	0.92 ± 0.27	4.79 ± 3.18	< 0.001

**Table 4.** Metabolite ratios (Mean ± SD) and their statistical significance in the basal ganglia, the dorsolateral prefrontal lobe, and the hippocampus of MCI patients

Basal ganglia		LCModel	SAGE	P value
	mI/Cr	0.74 ± 0.15	0.22 ± 0.17	< 0.001
	Cho/Cr	0.33 ± 0.08	0.28 ± 0.06	0.01
	NAA/Cr	1.03 ± 0.23	2.05 ± 0.54	< 0.001
	NAA/ml	1.43 ± 0.36	17.2 ± 20.7	< 0.001
Dorsolateral prefrontal lobe	mI/Cr	1.14 ± 0.35	0.48 ± 0.41	< 0.001
	Cho/Cr	0.45 ± 0.18	0.39 ± 0.19	0.08
	NAA/Cr	1.43 ± 0.34	2.34 ± 0.88	0.02
	NAA/ml	1.3 ± 0.26	7.51 ± 6.08	< 0.001
Hippocampus	mI/Cr	1.34 ± 0.14	0.43 ± 0.27	< 0.001
	Cho/Cr	0.41 ± 0.04	0.36 ± 0.1	0.07
	NAA/Cr	1.16 ± 0.23	2.45 ± 0.89	< 0.001
	NAA/ml	0.88 ± 0.2	7.44 ± 4.67	< 0.001

for all other ratios determined by the two methods. In the MCI patients, except for Cho/Cr in the DLPL and the hippocampus, significant differences ( $p < 0.05$ ) were found for all other ratios determined by the two methods.

## DISCUSSION

This study successfully determined the brain metabolite concentration ratios using LCModel and SAGE. In 1H MRS, the signal of metabolites may superimpose

with the baseline of macromolecular compounds. However, brain metabolites, such as mI, are valuable biomarkers for the early diagnosis of MCI diseases. Delayed acquisition can remove the interference signals of macromolecules; however, the mI signal may be lost due to the short T2 relaxation time. The area of resonance may be obtained by numerical integration. However, this method may cause significant under- or over-estimation of the resonance area due to resonance overlapping<sup>(18)</sup>. This is because individual peak areas cannot be accurately estimated by integration. Because fewer overlapping resonances are associated with phantom experiments, due to less macromolecular interferences as compared to in vivo experiments, the concentration ratios determined by LCModel or SAGE show insignificant differences. Furthermore, the NAA signal overlaps with the glutamate and macromolecular signals under shorter echo times. In addition, resonance from other N-acetyl-containing metabolites, such as N-acetylaspartylglutamate (NAAG), will essentially coincide with the NAA methyl signal, thereby further complicating the NAA quantification (24). In fact, our in vivo data showed that the NAA/Cr ratio determined by SAGE analysis was approximately two-folds of that calculated by LCModel.

Eddy currents, inhomogeneity of the magnetic field, and environmental factors cause complicated line broadening and peak overlap as well as severe peak distortion and baseline complications, which influence determination of the concentration ratios in vivo partly due to user-based subjectivity and bias. LCModel uses a nearly model-free method, attempting to choose the best compromise between peak distortion and baseline complications in finding the smoothest peak profile that fits the data via a fully automatic process without user interaction<sup>(19,20)</sup>. As shown in Figures 4 and 5, the spectra from an in vivo environment suffer from severe peak overlapping and distortion. Our results showed that the mI/Cr and NAA/Cr ratios were significantly overestimated ( $p < 0.05$ ) by SAGE analysis, even in the phantom experiment. This may increase the chance of artificial errors arising from the SAGE analysis. Our data, as calculated by SAGE, showed greater differences between the healthy controls and the MCI patient group as compared to the differences calculated by the LCModel. Therefore, we concluded that there were significant

differences ( $p < 0.05$ ) between the two methods.

Error estimates are important in reporting the determined concentration ratios. The Cramer–Rao lower bounds (CRLBs) error estimate is used in LCModel<sup>(21,22,23)</sup>, and metabolite ratios calculated with a CRLB  $> 15\%$  are discarded. Even for a calculated ratio with a CRLB  $< 15\%$ , the spectra quality still needs to be checked because poor spectra quality may cause artifacts or errors. However, the SAGE analysis method does not have an error estimate to indicate the spectra quality.

Peak overlapping and macromolecular interference are two major factors for the significant differences in the metabolite concentration ratios determined by LCModel and SAGE. At short echo times, Cho resonance overlapped with that of thanolamine myo-inositol, glucose, or taurine. NAA overlapped with that of glutamate, NAAG, and macromolecules at shorter echo times<sup>(24)</sup>. Behar et al.<sup>(25,26)</sup>, Kauppinen et al.<sup>(27,28)</sup>, and Hofmann et al.<sup>(29)</sup> have extensively studied macromolecular resonance in human and animal brains. According to their results, broad peak M5 and M8 may affect the accuracy of the concentration ratios. Compared to SAGE, the LCModel method is more capable of filtering these data based on its unique error estimate parameter.

Cho/Cr ratios estimated by LCModel and SAGE derived from the measurements of the basal ganglia, DLPL, the hippocampus of the healthy volunteers exhibited no statistically significant ( $p > 0.05$ ) differences. We confirmed that the spectra quality of Cho is better than that of the other metabolites, and this may have eliminated artificial errors caused by the SAGE method.

The difference of metabolite ratio between true concentration and analysis by LCModel and SAGE and their statistical significance are show in Table.2. The ratios of metabolite by LCModel analysis are close to true concentration than SAGE except mI/Cr. Although, there are no significant differences ( $p > 0.05$ ) but the results by LCModel are more close to true concentration than SAGE.

Finally, according to the report of Kantarci et al.<sup>(30,31)</sup>, the mI/Cr concentration was increased and the NAA/Cr concentration was decreased in the brains of the MCI patients as compared to healthy volunteers. However, such trends were not observed in our results, and further validation and experiments are required.

## CONCLUSION

The metabolite concentration ratios in brains determined by LCModel or SAGE were found to be acceptable and comparable. The LCModel, however, was marginally more accurate than SAGE due to its full automation, excellent processing capacity of peak overlapping and macromolecular interference, basis set and user independency.

## REFERENCES

1. Sachin K. Guja, Sharad Maheshwari, Isabella Bjo rnkman-Burtscher, Pia C. Sundgren. Magnetic Resonance Spectroscopy. *J Neuro-Ophthalmol* 2005; 25:217–226.
2. Rubaek Danielsen E, Ross B (eds.). Magnetic resonance spectroscopy diagnosis of neurological disease. New York. Marcel Dekker, Inc. 1999.
3. Burtscher IM, Holtas S. Proton MR spectroscopy in clinical routine. *J Magn Reson Imaging* 2001;13:560–567.
4. Castillo M, Kwock L, Mukherji SK. Clinical applications of proton MR spectroscopy. *AJNR Am J Neuroradiol* 1996;17:1–15.
5. Barker, PB. Fundamentals of MR spectroscopy. in: JH Gillard, AD Waldman, PB Barker (Eds.) *Clinical MR neuroimaging*. Cambridge University Press, Cambridge;2005:7–26.
6. Wang ZJ, Zimmerman RA. Proton MR spectroscopy of pediatric metabolic disorders. *NeuroImag Clin N Am* 1998;8:781–807.
7. Zimmerman RA, Wang ZJ. The value of proton MR spectroscopy in pediatric metabolic brain disorders. *AJNR Am J Neuroradiol* 1997;18:1872–1879.
8. Maheshwari SR, Fatterpekar GM, Castillo M, Mukherji SK. Proton MR spectroscopy of the brain. *Semin Ultrasound CT MR* 2000;21:434–451.
9. Miller BL, Moats R A, Shonk T, Ernst T, Woolley S, Ross B D. Alzheimer disease: depiction of increased cerebral myo-inositol with proton MR spectroscopy. *Radiology* 1993;187:433–437.
10. Shonk TK, Moats RA, Gifford P, Michaelis T, Mandigo JC, Izumi J, Ross BD. Probable Alzheimer disease: diagnosis with proton MR spectroscopy. *Radiology* 1995;195:65–72.
11. Kantarci K, Jack CR, Jr, Xu YC, Campeau NG, O'Brien PC, Smith GE, Ivnik RJ, Boeve BF, Kokmen E, Tangalos EG, Petersen RC. Regional metabolic patterns in mild cognitive impairment and Alzheimer's disease: A 1H MRS study. *Neurology* 2000;55:210–217.
12. Catani M, Cherubini A, Howard R, Tarducci R, Pelliccioli GP, Piccirilli M, Gobbi G, Senin U, Mecocci P. 1H-MR spectroscopy differentiates mild cognitive impairment from normal brain aging. *Neuroreport* 2001;12, 2315–2317.
13. Petersen RC, Smith GE, Ivnik RJ, Tangalos EG, Schaid DJ, Thibodeau SN, Kokmen E, Waring SC, Kurland LT. Apolipoprotein E status as a predictor of the development of Alzheimer's disease in memory impaired individuals *JAMA* 1995;273(16):1274–1278.
14. Smith GE, Petersen RC, Parisi JE, Ivnik RJ. Definition, course and outcome of mild cognitive impairment. *Aging, Neuropsychology and Cognition* 1996;3(2):141–147.
15. Martinez-Bisbal MC, Arana E, Marti-Bonmati L, Molla E, Celda B. Cognitive impairment: classification by 1H magnetic resonance spectroscopy. *Eur J Neurol* 2004;11:187–193.
16. Metastasio A, Rinaldi P, Tarducci R, et al. Conversion of MCI to dementia: Role of proton magnetic resonance spectroscopy. *Neurobiol Aging* 2006;27: 926–932.
17. GE Medical Systems. SAGE7 LX User's Guide.
18. Robin A. de Graaf. *In Vivo NMR Spectroscopy: Principles and Techniques*. 2007; Wiley.
19. Provencher SW. Automatic quantitation of localized in vivo 1H spectra with LCModel. *NMR Biomed* 2001; 14:260–264.
20. Provencher SW. Estimation of metabolite concentrations from localized in vivo proton NMR spectra. *Magn Reson Med* 1993;30:672–679.
21. Cavassila S, Deval S, Huegen C, van Ormondt D, Graveron-Demilly D. Cramer–Rao bound expressions for parametric estimation of overlapping peaks: influence of prior knowledge. *J Magn Reson* 2000;143:311–320.
22. Cavassila S, Deval S, Huegen C, van Ormondt D, Graveron-Demilly D. Cramer–Rao bounds: an

- evaluation tool for quantitation. *NMR Biomed* 2001; 14:278–283.
23. Ratiney H, Coenradie Y, Cavassila S, van Ormondt D, Graveron-Demilly D. Time-domain quantitation of  $^1\text{H}$  short echo-time signals: background accommodation. *Magma* 2004;16:284–296.
24. Frahm J, Michaelis T, Merboldt KD, Hancicke W, Gyngell ML, Bruhn H. On the N-acetyl methyl resonance in localized  $^1\text{H}$  NMR spectra of human brain in vivo. *NMR Biomed* 1991;4:201–204 (1991).
25. Behar KL, Ogino T. Characterization of macromolecule resonances in the  $^1\text{H}$  NMR spectrum of rat brain. *Magn Reson Med* 1993;30:38–44.
26. Behar KL, Rothman DL, Spencer DD, Petroff OA. Analysis of macromolecule resonances in  $^1\text{H}$  NMR spectra of human brain. *Magn Reson Med* 1994;32:294–302.
27. Kauppinen RA, Kokko H, Williams SR. Detection of mobile proteins by proton nuclear magnetic resonance spectroscopy in the guinea pig brain ex vivo and their partial purification. *J Neurochem* 1992;58:967–974.
28. Kauppinen RA, Niskanen T, Hakumaki J, Williams SR, Kauppinen RA, Kokko H, Williams SR. Quantitative analysis of  $^1\text{H}$  NMR detected proteins in the rat cerebral cortex in vivo and in vitro. *NMR Biomed* 1993;6:242–247.
29. Hofmann L, Slotboom J, Boesch C, Kreis R. Characterization of the macromolecule baseline in localized  $^1\text{H}$ -MR spectra of human brain. *Magn Reson Med* 2001;46:855–863.
30. Kantarci K, Jack CR Jr., Xu YC, Campeau NG, O'Brien PC, Smith GE, Ivnik RJ, Boeve BF, Kokmen E, Tangalos EG, Petersen RC. Regional metabolic patterns in mild cognitive impairment and Alzheimer's disease: A  $^1\text{H}$  MRS study. *Neurology* 2000 Jul 25;55(2):210–217.
31. Kantarci K, Xu Y, Shiung MM, O'Brien PC, Cha RH, Smith GE, Ivnik RJ, Boeve BF, Edland SD, Kokmen E, Tangalos EG, Petersen RC, Jack CR Jr. Comparative diagnostic utility of different MR modalities in mild cognitive impairment and Alzheimer's disease. *Dement Geriatr Cogn Disord* 2002;14:198–207.